



## Preparation and characterization of a bacterial cellulose/silk fibroin sponge scaffold for tissue regeneration



H.G. Oliveira Barud<sup>b</sup>, Hernane da S. Barud<sup>a,e,\*</sup>, Maurício Cavicchioli<sup>a</sup>, Thais Silva do Amaral<sup>a</sup>, Osmir Batista de Oliveira Junior<sup>b</sup>, Diego M. Santos<sup>c</sup>, Antonio Luis de Oliveira Almeida Petersen<sup>c</sup>, Fabiana Celes<sup>c</sup>, Valéria Matos Borges<sup>c</sup>, Camila I. de Oliveira<sup>c</sup>, Pollyanna Francielli de Oliveira<sup>d</sup>, Ricardo Andrade Furtado<sup>d</sup>, Denise Crispim Tavares<sup>d</sup>, Sidney J.L. Ribeiro<sup>a</sup>

<sup>a</sup> Institute of Chemistry – São Paulo State University – Unesp, P.O. Box 355, Araraquara, SP 14801-970, Brazil<sup>1</sup>

<sup>b</sup> School of Dentistry/Unesp, São Paulo State University – Unesp, Rua Humaitá, 1680, Zip code 14801-903, Araraquara, SP, Brazil<sup>2</sup>

<sup>c</sup> Gonçalo Moniz Research Center, FIOCRUZ, Av. Waldemar Falcão, 121, Zip code 40296-710, Salvador, BA, Brazil<sup>3</sup>

<sup>d</sup> University of Franca, Av. Dr. Armando Salles de Oliveira, 201, Zip code 14404-600, Franca, SP, Brazil<sup>4</sup>

<sup>e</sup> Laboratório de Química Medicinal e Medicina Regenerativa (QUIMMERA) – Centro Universitário de Araraquara (UNIARA), Araraquara, SP, Brazil

### ARTICLE INFO

#### Article history:

Received 1 October 2014

Received in revised form 3 April 2015

Accepted 8 April 2015

Available online 17 April 2015

#### Chemical compounds studied in this article:

D-Glucose (PubChem CID: 5793)

glycine (PubChem CID: 750)

L-Alanine (PubChem CID: 5950)

MTT (PubChem CID: 64965)

XTT (PubChem CID: 14195569)

#### Keywords:

Bacterial cellulose

Silk fibroin

Biocompatible materials

Nanocomposites

Scaffold

Tissue engineering.

### ABSTRACT

Bacterial cellulose (BC) and silk fibroin (SF) are natural biopolymers successfully applied in tissue engineering and biomedical fields. In this work nanocomposites based on BC and SF were prepared and characterized by scanning electron microscopy (SEM), infrared spectroscopy (FT-IR), X-ray diffraction (XRD) and thermogravimetric analysis (TGA). In addition, the investigation of cytocompatibility was done by MTT, XTT and Trypan Blue dye technique. Cellular adhesion and proliferation were detected additionally. The evaluation of genotoxicity was realized by micronucleus assay. *In vitro* tests showed that the material is non-cytotoxic or genotoxic. SEM images revealed a greater number of cells attached at the BC/SF:50% scaffold surface than the pure BC one, suggesting that the presence of fibroin improved cell attachment. This could be related to the SF amino acid sequence that acts as cell receptors facilitating cell adhesion and growth. Consequently, BC/SF:50% scaffolds configured an excellent option in bioengineering depicting its potential for tissue regeneration and cultivation of cells on nanocomposites.

© 2015 Elsevier Ltd. All rights reserved.

### 1. Introduction

Tissue engineering has the purpose of developing therapeutic options especially designed to be applied in special clinical conditions, aiming to replace or regenerate damaged tissues

using biomaterials. The success of the methodology depends on Biomaterials' properties that can be manipulated to mimic the three-dimensional architecture of extracellular matrix (ECM) native tissues which is regarded as a complex organization of fibrous structural proteins such as collagens and a wide variety of proteoglycans and polysaccharides (Cai & Xu, 2011; Shi et al., 2012, 2014).

In recent years, due to climate changes and the decrease of oil supply, synthetic materials are becoming increasingly unfavorable, enhancing the need to find renewable green alternatives. It is generally known that nanomaterials show unusual properties, not observed in the bulk materials, such as high surface reactivity and ability to cross-cell membranes. The development of materials with biomimetic behavior is essential for tissue engineering purposes

\* Corresponding author at: Institute of Chemistry – São Paulo State University – Unesp, P.O. Box 355, Araraquara, SP 14801-970, Brazil.

E-mail address: [hernane.barud@gmail.com](mailto:hernane.barud@gmail.com) (H.d.S. Barud).

<sup>1</sup> Tel.: +55 16 3301 9500.

<sup>2</sup> Tel.: +55 16 3301 9300.

<sup>3</sup> Tel.: +55 71 3176 2201.

<sup>4</sup> Tel.: +55 16 3711 8871.

because scaffolds based on nanofibres (NFs) mimic the natural extracellular matrix and its nanoscale fibrous structure (Barnes et al., 2008; Hutchens, Benson, Evans, O'Neill, & Rawn, 2006).

Cellulose is the most abundant biopolymer on earth and is present in a wide variety of living species being harvested mainly obtained from trees and cotton. It can also be obtained from the bacteria *Gluconacetobacter xylinus* that produces nano bacterial cellulose (BC) free of lignin and hemicellulose in a 3-D hierarchical network composed by bundles of much finer microfibrils of nanometric size range from 3.0 to 3.5  $\mu\text{m}$  (Barud et al., 2011; Klemm, Heublein, Fink, & Bohn, 2005; Svensson et al., 2005). Since its discovery BC has shown tremendous potential as an effective biopolymer in various fields, as the structural aspect of BC is far superior to those of plant cellulose, which provide it with better properties (Ul-Islam, Khan, & Park, 2012).

Then, BC is a completely biocompatible polymer also useful as scaffold for cellular growth and tissue engineering (Bäckdahl et al., 2006; Helenius et al., 2006; Rambo et al., 2008; Svensson et al., 2005). It is distinguished from the usual scaffolds because BC possesses natural refined 3-D nanofibrils networks bearing a shape similar to that of the collagen nanofibrils in natural tissue such as umbilical cord (Bäckdahl et al., 2006) and basement membrane in cornea (Fraser et al., 2008).

Due to this uniform structure and morphology BC is endowed with unique characteristics such as high purity, high crystallinity and remarkable mechanical properties, good chemical stability, and the high water holding capacity (Svensson et al., 2005). Despite its high water content, BC shows a good mechanical performance and BC can be produced in almost any shape because of its high moldability during formation (Ross, Mayer, & Benziman, 1991).

BC is used as a wound dressing since it provides a moist environment, resulting in better wound healing with no toxicity (Barud et al., 2007; Klemm et al., 2005). Besides that, BC offers a wide range of applications, especially in medical applications, artificial micro vessel, and tissue engineering of cartilage and bone (Fontana et al., 1990; Klemm, Schumann, Udhhardt, & Marsch, 2001; Svensson et al., 2005). Other studies with endothelial, smooth muscle cells and chondrocytes have shown that these cells present good adhesion to bacterial cellulose (Bäckdahl et al., 2006; Helenius et al., 2006; Rambo et al., 2008; Svensson et al., 2005).

However, some characteristics that would limit BC in medical applications is that BC is not easily absorbed in human body; in dried state BC nanofibrils form a dense mesh that can limit cell adhesion and proliferation (Bäckdahl et al., 2006). Besides that, BC has no antibacterial properties and acts only as a physical barrier against infection (Czaja, Young, Kawecki, & Brown, 2007).

Polymer composites have enhanced material and biological properties compared to pure polymers. Based on the nature and size of the reinforcement material, BC composites are synthesized through numerous routes aiming to overcome its limitations and increase its applications.

Literature displays several composites based on BC, such as BC/chitosan (Kim et al., 2011), BC/agarose (Yang et al., 2011), BC/poly(3-hydroxybutyrate)(PHB) (Barud et al., 2011; Barud, Caiut, Dexpert-Ghys, Messaddeq, & Ribeiro, 2012), BC/hydroxyapatite (Hap) (Grande et al., 2009; Saska et al., 2011) and BC/Collagen (Luo et al., 2008; Saska et al., 2012). These bacterial cellulose based materials have been commercialized and recognized as non-genotoxic and non-cytotoxic (Jonas & Farah, 1998; Schmitt, Frankos, Westland, & Zoetis, 1991). Among the investigated materials that could possibly be associated with BC, we have opted to use silk fibroin (SF).

Fibroin is a natural protein extracted from silk cocoons of *Bombyx mori* silkworm that can be processed to create a variety of materials such as hydrogels, ultrathin and thick films, 3D porous matrices, and fibers with controllable diameters (Omenetto &

Kaplan, 2010). This protein is also a potential candidate material for biomedical applications because it has several attractive properties, including good biocompatibility, good oxygen and water vapor permeability, and biodegradability (Altman et al., 2003; Wang, Blasioli, Kim, Kim, & Kaplan, 2006) that can be controlled by functionalization of fibroin or changing the processing methods.

SF reveals some known applications like the preparation of scaffolds for bone and meniscus regeneration (Altman et al., 2003; Bhardwaj et al., 2011; Kim, Jeong, et al., 2005; Kim, Park, Kim, Wada, & Kaplan, 2005; Mandal, Park, Gil, & Kaplan, 2011; Mauney et al., 2007; Zhang et al., 2010), small-diameter graft for vascular substitution (Alessandrino et al., 2008; Cattaneo et al., 2013; Enomoto et al., 2010; Marelli, Alessandrino, Fare, Tanzi, & Freddi, 2009; Marelli et al., 2010) and transparent thin films for biophotonics (Amsden et al., 2010).

In addition, SF as protein has amino acids that act as cell receptors and mediate important interactions between mammalian cells and extra cellular matrix (ECM) facilitating cell adhesion and growth (Fang, Chen, Yang, & Li, 2009; Fang, Wan, Tang, Gao, & Dai, 2009) and it presents antimicrobial activity (Li et al., 2011). However, the regenerated SF has some disadvantages, such as brittleness, easy fragmentation, and difficulty in creating a uniform thickness (Lee, Kim, Lee, & Park, 2013).

Some authors have prepared plate BC/SF composites and observed the improvement of the mechanical properties of SF (Choi, Cho, Heo, & Jin, 2013) and others applied them in an animal model to promote the complete healing of segmental defects of zygomatic arch (Lee et al., 2013) without previously studying it *in vitro*. Despite both materials being separately biocompatible, it is important to demonstrate if this new composite can be safely applied in tissue regeneration.

Thus, the aim of this study was to prepare porous scaffolds based on BC and SF by lyophilization process, in order to maintain their properties and complement each other as a composite, taking advantage of BC's surface modification with amino acids extracted from SF. Toward meeting these objectives, the resultant nanocomposites were characterized by physicochemical techniques and the cytocompatibility was assessed by the investigation of the cytotoxicity and genotoxicity of the developed material.

## 2. Experimental

### 2.1. Materials

#### 2.1.1. Bacterial cellulose

Bacterial cellulose membranes were obtained from cultivation of the *Gluconacetobacter hansenii* strain ATCC 23769. Cultures were incubated for 96 h at 28 °C in trays 30 cm × 50 cm, containing medium composed of glucose 50 g L<sup>-1</sup>, yeast extracts 4 g L<sup>-1</sup>, anhydrous disodium phosphate 2 g L<sup>-1</sup>, heptahydrated magnesium sulphate 0.8 g L<sup>-1</sup> and ethanol 20 g L<sup>-1</sup>. After three days of incubation hydrated BC pellicles of 3 mm of thickness containing up to 99% of water and 1% of cellulose were obtained. These membranes were washed in a 1 wt% aqueous NaOH at 70 °C in order to remove bacteria and then several times in water, until neutral pH. Pristine bacterial cellulose membranes (25 cm<sup>2</sup>) were used for nanocomposite preparation.

#### 2.1.2. Silk fibroin solution

Silk fibroin (SF) solution was obtained from silk cocoons produced by *Bombyx mori* silk worms supplied by Bratac, Fiaçao de Seda S.A. (Bastos/SP, Brazil). The method was based on previous reports from literatures (Kweon, Ha, Um, & Park, 2001; Rockwood et al., 2011). Raw silk was degummed with 0.02 M Na<sub>2</sub>CO<sub>3</sub> solution at 100 °C for 30 min and washed thoroughly with distilled water. Degummed silk was dissolved in a solution composed of CaCl<sub>2</sub>, H<sub>2</sub>O,

and ethanol (1:8:2 molar ratio) in a proportion of 1 g of silk to 4 mL of the solvent. The resulting viscous solution was dialyzed against mili-Q water for 48 h in order to remove salts. A 3.7% (w/V) aqueous fibroin solution free of impurities was obtained after the centrifugation (twice) of the dialyzed solution at 20,000 rpm at 4 °C for 30 min. The final concentration of aqueous SF solution (3.7 wt.%) was determined by weighing the dried solids. The final solution was stored at 4 °C before use. The stock fibroin solution (3.7%) was used to prepare BC/fibroin composites.

### 2.1.3. Bacterial cellulose/silk fibroin nanocomposites

Porous composites of BC/SF were prepared by soaking BC membranes (25 cm<sup>2</sup>) into silk fibroin solutions of different concentrations (1%, 3% and 7% of SF content (w/v) in order to exchange water by the silk fibroin solution into the microfibrillar cellulose's network. The membranes were kept in fibroin solutions for 24 h under shaking, removed and freeze dried.

The final SF contents in BC/SF nanocomposites were determined by the mass percentages of SF. The remaining SF in solution was measured and subtracted from the initial SF amount in order to calculate SF bound to the BC membranes. Samples were termed according to SF contents BC/SF:25%, BC/SF:50% and BC/SF:75%. They were all packed and sterilized with a 25 kGy gamma irradiation (Embrarad – Brazil).

### 2.2. Field emission scanning electron microscopy

Scanning electron microscopy (SEM) images were obtained with the use of a Field Emission Scanning Electron Microscope JEOL JSM–7500F. Freeze-dried scaffolds were carefully sectioned at horizontal plane with a razor blade, mounted with conductive adhesive tape on copper stubs, and sputter-coated with a carbon layer.

### 2.3. Solubility test

BC/SF nanocomposites were cut into pieces of 1.0 cm<sup>2</sup>, weighed ( $m_i$ ), immersed in 20 mL of distilled water and kept at 37 °C for 24 h. After this period, the samples were dried and weighed again ( $m_f$ ). The percentage of soluble mass was determined by the following equation. All experiments were performed in triplicate, and standard deviation was calculated.

$$\text{Soluble mass (\%)} = \frac{(m_i - m_f)100}{m_i}$$

### 2.4. Water-uptake capacity

The swelling ratio was calculated by placing separately pristine freeze-dried BC and BC/SF:50% samples of 1.0 cm<sup>2</sup> in distilled water for a specific time. Samples were removed at certain times, initially at 1 and 5 min, followed by measurements every 5 min up to 30 min, and then 60, 360 and 1440 min. After removal from the distilled water, excess superficial water was removed by gentle tapping with filter paper; then the samples were weighed. The content of the distilled water in the swollen scaffolds was calculated by the following equation: water uptake (%) = [( $W_s - W_d$ )/ $W_s$ ] × 100, where  $W_d$  is the weight of the dry membrane and  $W_s$  is the weight of the swollen membrane, respectively. All experiments were performed in triplicate, and standard deviation was calculated.

### 2.5. Measurement of SF release with time

The fibroin protein concentration was measured by the Bradford protein assay procedure (Bradford, 1976), in order to investigate the stability of scaffolds in aqueous environment. Samples of 1.0 cm<sup>2</sup> BC/SF:50% scaffolds were immersed in 5 mL of deionized water.

The Bradford reagent was added and the samples were incubated at 30 °C, in the dark. The aliquots were collected at 5, 15, 30, 60, 720 and 1440 min. The Bradford assay relies on the binding of the dye Coomassie Blue G-250 to protein. Therefore, the quantity of protein can be estimated by determining the amount of dye in the blue ionic form, usually achieved by measuring the absorbance of the solution at 595 nm. Bovine serum albumin was used as a standard protein.

### 2.6. FT-IR spectroscopy

Infrared spectra were recorded on a Spectrum 2000 FT-IR Perkin Elmer spectrophotometer, using samples prepared as KBr pellets. The spectra were collected over the range of 4000–700 cm<sup>-1</sup> with an accumulation of 32 scans, resolution of 2 cm<sup>-1</sup> and interval of 0.5 cm<sup>-1</sup>.

### 2.7. Thermogravimetric analysis

Thermogravimetry (TG) was conducted using dried samples on a Thermoanalyzer TG/DTA simultaneous SDT 2960 TA Instruments under the following conditions: aluminum crucible, synthetic air (100 mL/min), and a heating rate at 10 °C per minute, from 30 to 1000 °C.

### 2.8. Powder X-ray diffractometry

X-ray diffraction patterns (XRD) were obtained in a Siemens Kristalloflex diffractometer using nickel filtered Cu K- $\alpha$ -radiation from 4° to 70° (2θ angle), in steps of 0.02° and a step time of 3 s.

### 2.9. Porosity study

A porosity study was conducted by examining SEM surface images of the composite that will be used to perform *in vitro* tests applying *Image J* software. The calculation was based on 30 diameter measurements of different pores to estimate average, coefficient of variation and confidence level of data obtained.

### 2.10. Cytotoxicity and genotoxicity assays

These tests were performed only in case of BC/SF:50% samples. Cytotoxicity can be measured by multiple different methods depending on the cell damage: changes in plasma membrane are detected by using dyes, such as Trypan Blue, and changes related to metabolic functions of mitochondria can be detected by a colorimetric method such as MTT (tetrazolium 3-(4,5-dimethylthiazol-2-yl)-2,5-diphenyl tetrazolium bromide) (Kim, Yoon, Lee, & Jeong, 2009) and XTT (2,3-bis[2-methoxy-4-nitro-5-sulfophenyl]-2H-tetrazolium-5-carboxanilide), according to the manufacturer's instructions.

Thus, the cytotoxicity assay requires a selection based on the suitability of the cell employed in the test method. The present study used L929 cells for the MTT test which is in accordance with ISO standards (10993-5:2009) and Chinese hamster fibroblasts (V79 cells) for the XTT method according to ISO 10993-12:2007 that goal *in vitro* cytotoxicity tests of biomedical devices.

#### 2.10.1. Preparation of the samples for *in vitro* tests

As mentioned in Section 2.1.3, freeze dried BC and BC/SF:50% scaffolds previously sterilized were then soaked in RPMI 1640 medium (Invitrogen) for 1 h in 24-well plates to facilitate cell adhesion. L-929 cells were lifted with trypsin/EDTA (Invitrogen), washed twice with saline by centrifugation, seeded onto the scaffolds (10 µL/scaffold at 5 × 10<sup>5</sup> cells/mL), and allowed to attach for 1 h at 37 °C, 5% CO<sub>2</sub>. One mL of RPMI medium supplemented with 2 mM L-glutamine, 100 U/mL penicillin, 100 µg/mL streptomycin,

10% FCS (all from Invitrogen<sup>TM</sup>) and 0.05 M  $\beta$ -mercaptoethanol was added to wells and cells were cultivated for 48 h. All treatments, negative control and also positive control were performed in quintuplicate and in conditions of sterility.

The V79 cell line was maintained and cultivated as monolayers in plastic culture flasks ( $25\text{ cm}^2$ ) containing HAM-F10 plus DMEM (1:1; Sigma–Aldrich), supplemented with 10% fetal bovine serum (Nutricell) and 2.38 mg/mL Hepes (Sigma–Aldrich) at  $37^\circ\text{C}$  in a humidified 5%  $\text{CO}_2$  atmosphere. Antibiotics (0.01 mg/mL streptomycin and 0.005 mg/mL penicillin; Sigma–Aldrich) were added to the medium to prevent bacterial growth. The BC/SF:50% was extracted with HAM-F10 plus DMEM (1:1) for 72 h at  $37^\circ\text{C}$  and sonicated for 1 h before treatment. Immediately prior to use, the culture medium was transferred to another flask and fetal bovine serum was added up to volume. This solution was set as a reference as 100%.

#### 2.10.2. MTT assay

After the preparation, the samples were removed from each well and the cultures were washed with 250  $\mu\text{L}$  of saline solution. With the laminar flow light off, 200  $\mu\text{L}$  of M199 medium (Invitrogen<sup>TM</sup>) without phenol red solution with MTT (final concentration 500  $\mu\text{g}/\text{mL}$ ) were placed per well. The plates were incubated at  $37^\circ\text{C}$  for a treatment period of 4 h. Then, the colorimetric measurement was verified with spectrophotometer spectra Max 190 (Molecular Devices) at 570 nm and 690 nm, and the result allows an Optical Density measurement (OD) analysis. The darker the color, the higher the metabolism of MTT and consequently, the higher the OD and less cytotoxic is the material tested.

#### 2.10.3. Trypan Blue assay

Trypan Blue Solution is routinely used as a stain to assess cell viability using the dye exclusion test. This test is often performed while counting cells with the hemocytometer during routine subculturing, but can be performed any time cell viability needs to be determined quickly and accurately. The dye exclusion test is based upon the concept that viable cells do not take up impermeable dyes (like Trypan Blue), but dead cells are permeable and take up the dye. After the initial preparation (see Section 2.10.1), the percentage of viable cells was determined by counting 200 cells in at least five random fields using the inverted light microscope in the presence of 50  $\mu\text{L}$  of Trypan Blue.

#### 2.10.4. XTT assay

For this experiment,  $10^4$  cells were plated onto 96-well microplates. Each well received 100  $\mu\text{L}$  HAM-F10/DMEM containing different percentages of BC/SF:50% ranging from 0.78% to 100%. The cells were cultured in a 5%  $\text{CO}_2$  atmosphere for 24 h at  $37^\circ\text{C}$ . After incubation, the culture medium was removed and the cells were washed with 100  $\mu\text{L}$  phosphate-buffered saline (PBS) and exposed to 100  $\mu\text{L}$  HAM-F10 culture medium without phenol red. Next, 25  $\mu\text{L}$  XTT (Roche Diagnostics) was added to each well and the microplates were incubated for 17 h at  $37^\circ\text{C}$ . Absorbance of the samples was read in a microplate reader (ELISA, Asys UVM 340/Microwin 2000) at a wavelength of 450 nm and a reference length of 620 nm. The amount of soluble product formed (formazan) was proportional to the number of viable cells. The negative control group was designated as 100%, and the results were expressed as a percentage of the negative control. Cytotoxicity was calculated with the GraphPad Prism program, plotting cell survival against the respective percentages of material. One-way ANOVA was used for the comparison of means ( $p < 0.05$ ). The experiments were performed in triplicate.

#### 2.10.5. Cell adhesion and proliferation assays

After the initial preparation, the number of cells seeded on the scaffolds was determined by counting in a Newbauer hemocytometer chamber by treatment with trypsin/EDTA. Scaffolds were then collected and the cell culture washed twice with RPMI 1640 medium (Invitrogen). Cells were fixed in a solution of 2.5% glutaraldehyde grade II, 2% formaldehyde and 2.5 mM  $\text{CaCl}_2$  in 0.1 M sodium cacodylate buffer pH 7.0 and processed for the preparation of SEM.

Regarding cell proliferation, treatments were performed in contact with the cells (at the following experimental periods: 16, 24, 48 and 72 h) by placing a disk of about 0.8 cm diameter of the biomaterials in each well. After the respective periods, cells were removed from the wells with trypsin-EDTA 0.25% V/V (GIBCO), centrifuged at  $1300 \times g$  rpm and  $40^\circ\text{C}$  for 10 min, resuspended in 20  $\mu\text{L}$  of Trypan Blue and then counted in a Newbauer hemocytometer chamber.

#### 2.10.6. Assessment of genotoxicity

The micronucleus assay in V79 cells was employed to evaluate the genotoxicity of BC/SF:50% samples. Therefore, 500,000 cells were seeded into tissue-culture flasks and incubated for 24 h in 5 mL completed HAM-F10/DMEM medium and washed with PBS (pH 7.4). After these procedures, the cultures were treated in serum-free medium for 3 h with three different percentages of BC/SF:50% (25%, 50% and 100%). We included the negative (without treatment) and positive (MMS – methyl methanesulfonate, 44  $\mu\text{g}/\text{mL}$ ) control groups. The cell cultures treated only with BC (100%) were also included. After the treatment period, the cells were washed with PBS and a culture medium supplemented with fetal bovine serum containing 3  $\mu\text{g}/\text{mL}$  of cytochalasin-B (CAS: 14930–96–2; Sigma–Aldrich) and the cells were incubated for 17 h. After the incubation, the cells were rinsed with 5 mL PBS, trypsinized using 0.025% trypsin-EDTA and centrifuged for 5 min at 900 rpm. The pellet was hypotonized in sodium citrate 1% at  $37^\circ\text{C}$  and then homogenized with a Pasteur pipette. This cell suspension was centrifuged again, the supernatant was discarded, the pellet was resuspended in methanol: acetic acid (3:1) and homogenized again with a Pasteur pipette. After fixation, the cells were stained in a Giemsa solution 5%. The criteria employed for the analysis of micronucleus were established by Fenech (2000). Therefore, 1000 binucleated cells were analyzed by culture in a total of 3000 binucleated cells per treatment. The nuclear division index (NDI) was determined for 500 cells analyzed per culture, for a total of 1500 cells per treatment group. Cells with well-preserved cytoplasm containing 1–4 nuclei were scored and the NDI was calculated using the following formula (Eastmond & Tucker, 1989):

$$IDN = \frac{[M1 + 2(M2) + 3(M3) + 4(M4)]}{N}$$

where  $M1–M4$  is the number of cells with 1, 2, 3, and 4 nuclei, respectively, and  $N$  is the total number of viable cells.

### 3. Results and discussion

#### 3.1. Infrared spectroscopy

FT-IR spectra for BC, SF and all BC/SF nanocomposites are shown in Fig. 1. The spectrum obtained for BC Fig. 1(a) shows bands in the 400–700  $\text{cm}^{-1}$  range characteristics of the OH bending,  $\beta$ -glucosidic linkages between the glucose units at  $\sim 896\text{ cm}^{-1}$  and C–O symmetric stretching of primary alcohol and C–O–C antisymmetric bridge stretching at  $1040\text{ cm}^{-1}$  and  $1168\text{ cm}^{-1}$ , respectively. The C–H deformation ( $\text{CH}_3$  or O–H in plane bending) is observed at  $1340\text{ cm}^{-1}$  and the band centered at  $1400\text{ cm}^{-1}$  is related to  $\text{CH}_2$  bending and OH in plane bending. According to Barud et al. (2008),

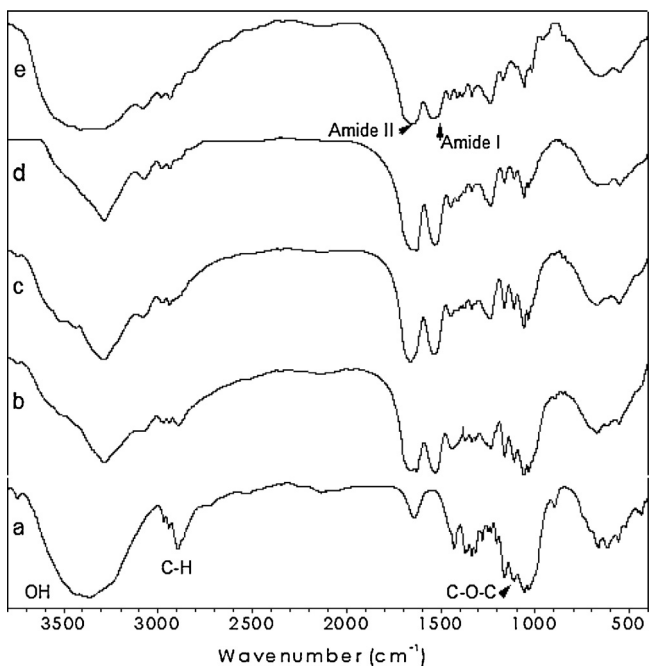


**Fig. 1.** FT-IR spectra: (a) pure freeze dried BC membrane, (b) freeze dried BC/SF composite (25% SF), (c) freeze dried BC/SF composite (50% SF), (d) freeze dried BC/SF composite (75% SF) and (e) pure freeze dried SF.

other bands are related to H—O—H bending of adsorbed water (at  $1650\text{ cm}^{-1}$ ), CH stretching of  $\text{CH}_2$  and  $\text{CH}_3$  groups (at  $2900\text{ cm}^{-1}$ ) and OH stretching (broad band at  $3500\text{ cm}^{-1}$ ).

The obtained spectra related to pure silk fibroin, Fig. 1(e), present bands in the region from  $1500$  to  $1700\text{ cm}^{-1}$  assigned to absorption by the peptide backbones of amide I ( $1700$ – $1600\text{ cm}^{-1}$ ) and amide II ( $1500$ – $1600\text{ cm}^{-1}$ ), which have been commonly used for the analysis of different secondary structures of fibroin. The peaks at  $1610$ – $1630\text{ cm}^{-1}$  (amide I) and  $1510$ – $1520\text{ cm}^{-1}$  (amide II) are characteristic of silk II ( $\beta$ -pleated sheet) secondary structure while the absorptions at  $1640$ – $1660\text{ cm}^{-1}$  (amide I) and  $1535$ – $1542\text{ cm}^{-1}$  are indicative of silk I ( $\alpha$ -form) conformation (Lu et al., 2011; Nazarov, Jin, & Kaplan, 2004). In the present study the amide I band of freeze dried fibroin showed strong peaks at  $1647$  and  $1537\text{ cm}^{-1}$  corresponding to silk I structure. However a shoulder at  $1620\text{ cm}^{-1}$  indicates the formation of some silk II.

For all BC/SF composites, cellulose bands in the region  $1000$ – $1300\text{ cm}^{-1}$  are exactly observed at the same positions and same relative intensities as pristine BC spectra shows. There are no important bands changing after silk fibroin impregnation in the nanocomposites. In fact FTIR spectra for all BC/SF nanocomposites could be considered only a sum of the BC and silk fibroin spectra and no new covalent bonds were detected, according to Kweon et al. (2001).

### 3.2. X-ray diffraction analysis

Fig. 2 shows XRD patterns for all samples. Broad diffraction peaks are observed at  $15^\circ$  and  $22.5^\circ$  for the pure BC membrane. These peaks are assigned to the characteristic interplane distances of native cellulose type 1 (Kim, Jeong, et al., 2005; Kim, Park, et al., 2005).

Freeze dried SF presents peaks at  $11.8^\circ$ ,  $19.8^\circ$  and  $22.6^\circ$  corresponding to the Silk I crystalline phase. The broad peaks should be due to the freeze drying process (Ming & Zuo, 2012).

Typical cellulose type I patterns are preserved in the BC/SF 25% nanocomposite, Fig. 2(b), and there are no significant changes when

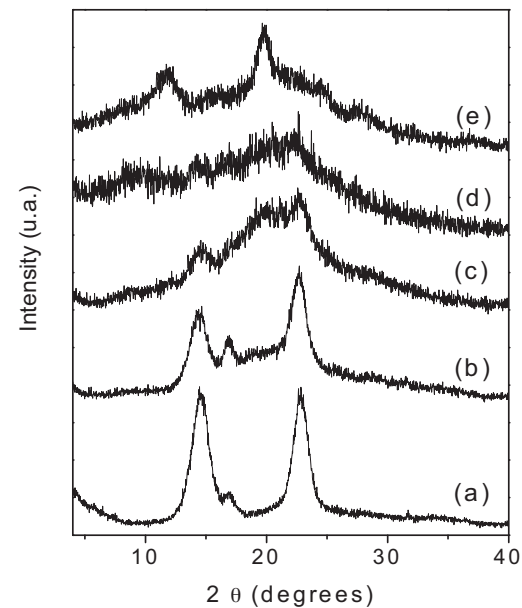


**Fig. 2.** XRD diffraction patterns: (a) pristine freeze dried BC, (b) freeze dried BC/SF composite (25% SF), (c) freeze dried BC/SF composite (50% SF), (d) freeze dried BC/SF composite (75% SF) and (e) pure freeze dried SF.

compared to the pristine BC diffractogram. Fig. 2 shows diffraction patterns characteristics of the superimposition of BC and SF pattern as observed. BC diffraction patterns overlap the SF pattern in the composites as observed by Lee et al. (2013). So, it is not possible to elucidate the type of SF crystal pattern (silk I or silk II) in these composites. XRD diffractogram for BC/SF:75% nanocomposites comprises an amorphous profile probably due to the large amount of silk fibroin deposited inside the BC porous as observed below in SEM images.

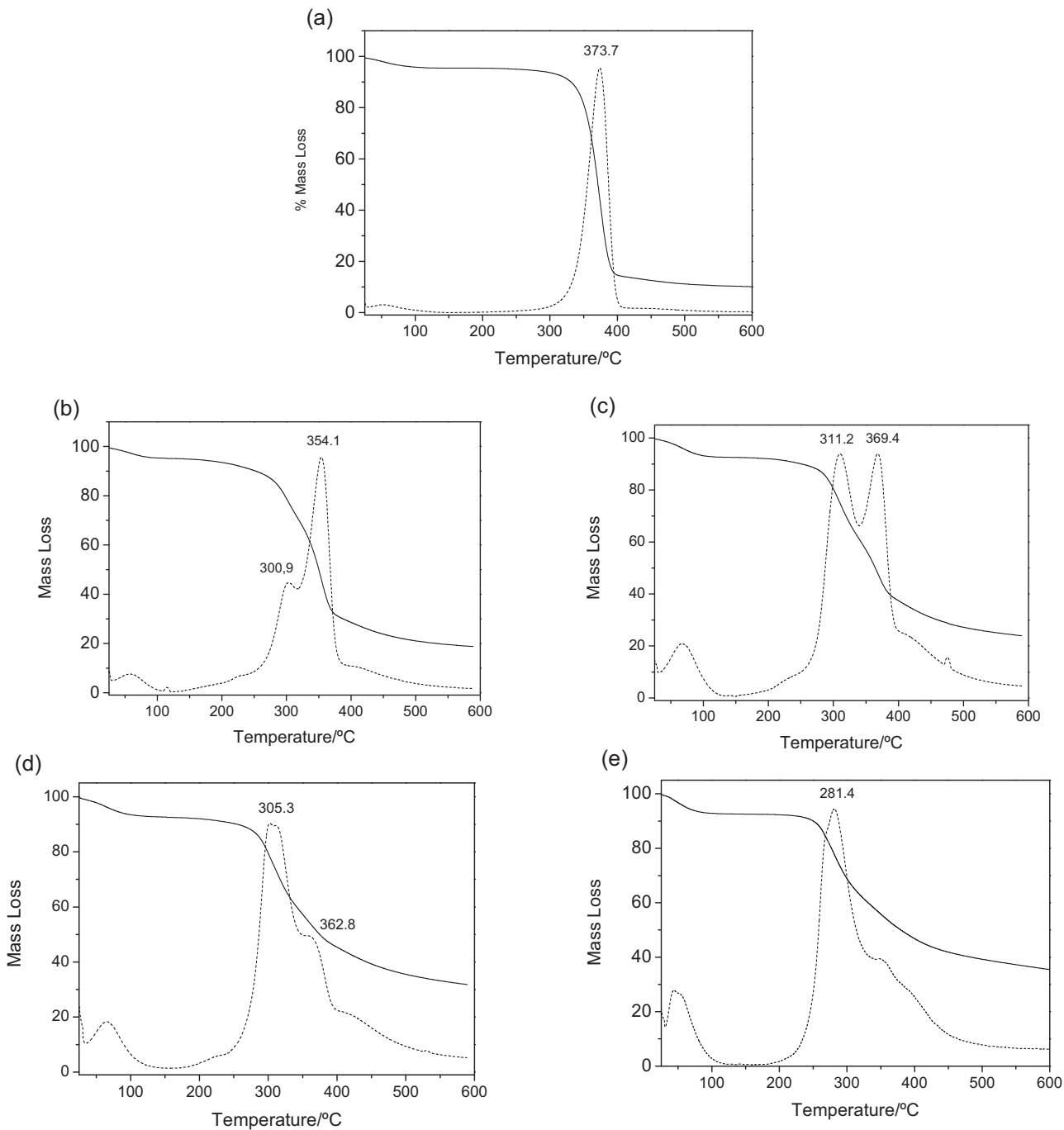
### 3.3. Thermogravimetric analysis

Fig. 3 shows TG/DTG curves. The curve obtained for freeze dried BC displays two mass losses. The first one, occurring from room temperature to  $200^\circ\text{C}$  is due to evaporation of the surface water ( $\sim 4.6\%$ ) (De Salvi, Barud, Caiut, Messadeq, & Ribeiro, 2012). The second more significant event related to a high mass loss (80%) begins at about  $280^\circ\text{C}$ , with maximum decomposition ( $T_{\text{onset}}$ ) at  $373.7^\circ\text{C}$ . This event is associated to thermal degradation, related to depolymerization and decomposition of dehydrocellulose into gases (water, carbon monoxide and carbon dioxide) (Sofia, McCarthy, Gronowicz, & Kaplan, 2001).

The initial mass loss for freeze dried SF is related to water loss and starts from room temperature to  $120^\circ\text{C}$  (7.3%). The second event involving mass loss (52%) occurs in the temperature range of  $180$ – $500^\circ\text{C}$  with maximum decomposition ( $T_{\text{onset}}$ ) at  $281.4^\circ\text{C}$ . This event is associated with the breakdown of side chain groups of amino acid residues, as well as the cleavage of peptide bonds (Nogueira et al., 2009).

TG curves obtained for BC/SF composites present three most important mass losses and display a composition of the events observed for the individual BC and SF components.

The first one is a continuous mass loss of around 7% from room temperature up to around  $200^\circ\text{C}$  which is associated with the water losses and is present in all BC/SF curves. Next, two major events in the range of  $200$ – $500^\circ\text{C}$  are present in all samples. The first one is attributed to fibroin decomposition counterparts and the second refers to BC decomposition.



**Fig. 3.** TG curves: (a) pristine freeze dried BC, (b) freeze dried BC/SF composite (25% SF), (c) freeze dried BC/SF composite (50% SF), (d) freeze dried BC/SF composite (75% SF) and (e) pristine freeze dried SF.

The DTG peak area is directly proportional to mass variations and could be used to compare the ratios between peaks heights for all composites. The first DTG peak, which is associated with the fibroin decomposition, becomes more intense when SF contents increase in nanocomposite. BC/SF:50%, Fig. 3(c) shows the same peak height for the first and second DTG peaks; it is quite relevant due to the BC and SF percentage ratio is of BC/SF 50:50 in this composite. In the same way the TG/DTG curve for BC/SF:75% sample denotes great similarity with the TG/DTG of the pristine fibroin. The height of the first DTG peak associated with the fibroin decomposition is larger than the first peak attributed to BC decomposition. These results corroborate with the gravimetric measurements whereby the percentage of the BC 25:75 fibroin in

this nanocomposite was determined. This behavior is due to higher SF content in this sample.

TG/DTG results also indicate that BC and SF decomposition events occur separately, and weak interactions between BC and SF suggested in FTIR analysis are therefore confirmed.

### 3.4. Field emission scanning electron microscopy (FEG-SEM)

SEM images are presented in Fig. 4. Surface images show that freeze-dried BC exhibits a 3-D network nanofibrils in the form of a heterogeneous porous structure that is observed in Fig. 4(a). These porous structures of BC sponges are similar to that of collagen sponges reported by Mizuno, Watanabe, and Takagi (2004).

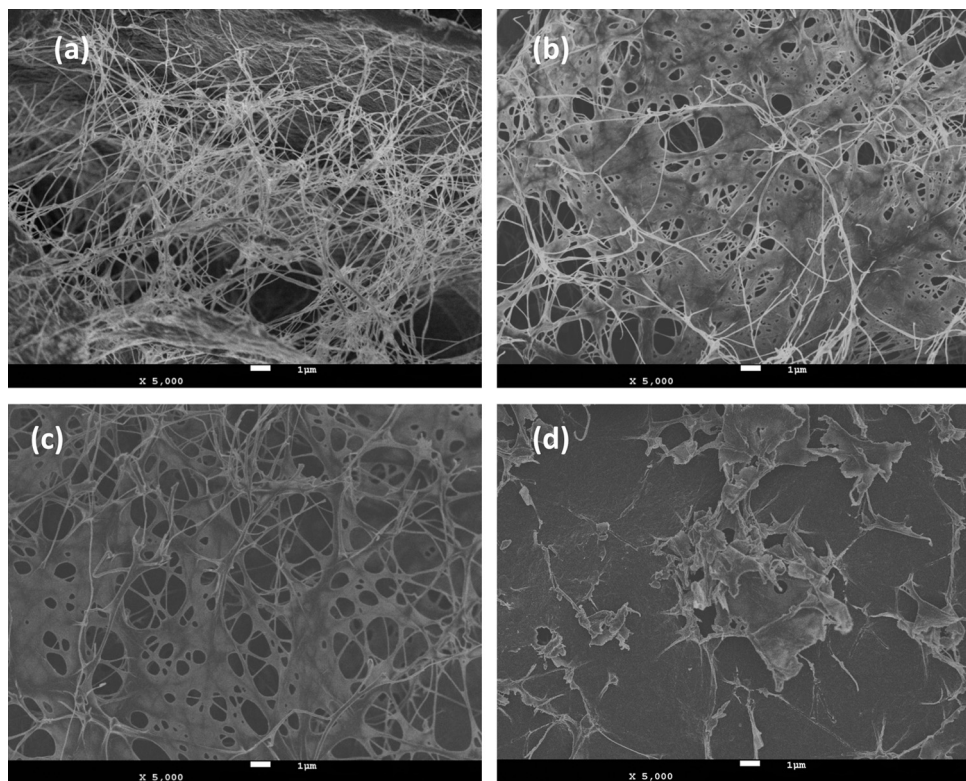


**Fig. 4.** FEG-SEM images taken at the same magnification (bar – 1  $\mu\text{m}$ ): (a) pure freeze dried BC, (b) freeze dried BC/SF 25% composite, (c) freeze dried BC/SF 50% composite and (d) freeze dried BC/SF 75%.

It is important to note that the method employed for BC cultivation could alter the morphology and porosity of the final cellulose membrane.

SEM images for BC/SF:25% and 50% nanocomposites reveal a sponge-like structure where BC nanofibers and fibroin structures are easily discerned. BC/SF samples exhibit a very well interconnected porous network structure formed by random nanofilaments entangled with each other presenting a large aspect surface. These characteristics also suggest that the presence of fibroin has modified the surface of BC nanocomposites and this modification may be induced by fibroin concentration. SEM image for BC/SF:75% sample presented a less porous structure due to the coating of the BC nanofibrils by excess of the SF solution.

Then, the best outcome obtained in this study was the one with 50% of SF and 50% of BC content. The result of this blend of 50% of each biomaterial results in a composite that is intended to preserve BC and SF properties.

### 3.5. Porosity study

In total 30 diameter measurements of different pores by examining SEM surface images of BC/SF:50% composites were examined. After statistical analysis the results revealed a pore size range of  $102 \pm 5.43 \mu\text{m}$  at the surface of the scaffolds.

As a scaffold for tissue engineering, macropores are required to allow for cell incorporation, migration, proliferation and tissue growth into the scaffold, according to Chen et al. (2002). But, on the other hand the literature also demonstrates that there is no general consensus regarding the optimal pore size for cell growth and tissue formation. Zeltinger, Sherwood, Graham, Mueller, and Griffith (2001) found that vascular smooth muscle cells showed equal cell proliferation and ECM formation in pores ranging in size from 38 to 150  $\mu\text{m}$ . Zhang et al. (2010) showed that pore sizes ranging from 100 to 300  $\mu\text{m}$  displayed human bone marrow mesenchymal

stromal cells (BMSCs) proliferation and ECM production applying silk fibroin scaffolds. These authors also observed that even in the presence of small pores of 50–100  $\mu\text{m}$  range there were BMSCs proliferation and ECM production occurred, but in less quantity.

In terms of porosity of BC/SF:50% scaffolds, our findings ( $102 \pm 5.43 \mu\text{m}$ ) are in accordance with these previous observations and also with Bhardwaj and Kundu (2011). They prepared SF/Chitosan and pure SF scaffolds for tissue regeneration and in terms of porosity results in a range of 100–155 and 90  $\mu\text{m}$  were identified.

One obvious challenge of tissue engineering is the design and fabrication of the 3-D polymer scaffolds composed of refined nanofibrils with hierarchical pore structure including large pores and nano pores to mimic the organization of ECMs (Kim et al., 2011). Gao et al. (2011) produced BC sponges by freeze-drying technique, with large and nano pores with a high surface area and they demonstrated that the material exhibited excellent cell compatible as fibrous synovium derived MSCs could proliferate well and grow inside the BC sponges.

Thus the results obtained in this study further supported by the literature lead us to conclude that the produced scaffolds could support BMSCs proliferation and ECM production, as the pore sizes of a scaffold matrix affect the cell adhesion, proliferation and directional growth, according to Bodin et al. (2010).

### 3.6. Water solubility test

Pristine SF sponge presents about 35.4% of solubility in water, in a period of 24 h. On the other hand, probably SF became more insoluble in contact with BC nanofibrils. Thus, BC/SF:25% nanocomposite presented 0% of solubility in distilled water, BC/SF:50%, 3.0%, and BC/SF:75%, 8.6%, as presented in Fig. 5(a). The increase on SF releasing may be related to the excess of SF attached to nanocomposites surface, as observed by SEM images.

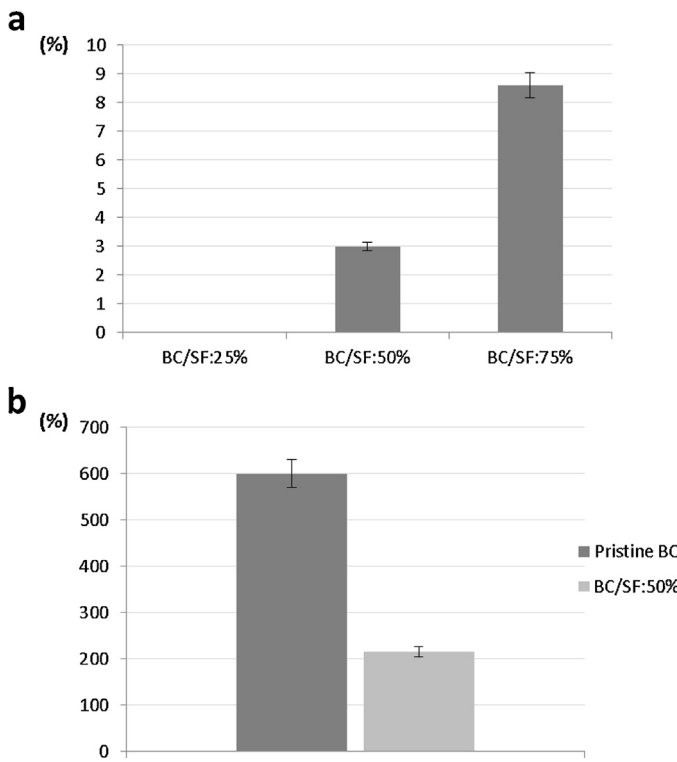


**Fig. 5.** (a) Water solubility test and (b) water-uptake capacity, expressed in percentage (%).

### 3.7. Water-uptake capacity

The water-uptake capacity is important to check if the material has the property to diffuse water, since the water diffusion allows the transport of nutrients, and helps the growth of new cells. The results showed that after 24 h, the water uptake ability of the pristine BC and BC/SF:50% scaffolds were about 600% (Klemm et al., 2001) and 216%, respectively (Fig. 5(b)). All the scaffolds absorbed water within 1 min; and they were saturated within 1 h. This behavior is due to the unique chemical and physical structures of BC and SF. There is diminishing on the swelling ability observed for BC/SF:50% scaffold. This decrease in the capacity of absorption may be related to the reduction of the amounts of BC pores due to SF presence, that had covered and obliterated BC surface, as SEM images show in Fig. 4.

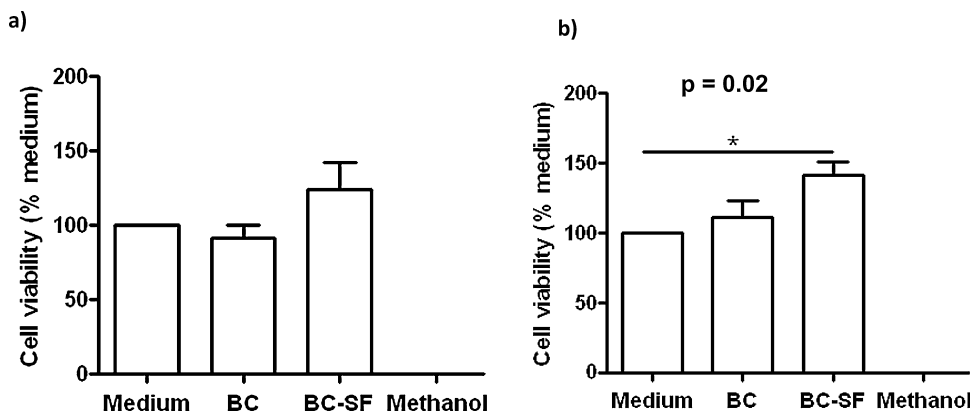


**Fig. 6.** Cell viability: (a) MTT method (group/medium) and (b) Trypan blue method (group/medium), expressed as a percentage (%).

### 3.8. Measurement of SF release with time

The Bradford assay demonstrated that no significant amount of silk fibroin protein was released to the solution in the initial measurements. After 24 h the final concentration of released protein was 0.89 mg/mL. Regarding the amount of protein released we believe that it may be related to the excess of silk fibroin attached to the scaffold since the amount of protein in solution has not changed after 24 h, indicating that BC/SF:50% scaffold remained stable in aqueous environment. Our results are in accordance with Sah and Pramanik (2010) that observed that after 3 h the concentration of silk fibroin released in solution was about 1.7 mg/mL. They show that the concentration of released protein did not change after 3 h, remaining stable.

### 3.9. Cytotoxicity and genotoxicity assays

The statistical analysis was performed according to Kruskal Wallis and Dunns in relation to MTT and Trypan Blue tests and Mann Whitney for cell adhesion and proliferation, by applying the statistical program Graphpad Prism 5.0. All *in vitro* tests results were statistically significant at  $p < 0.05$ .

#### 3.9.1. MTT assay

Colorimetric measurements were performed as the method described.

In terms of cell viability for 48 h by MTT, under the experimental conditions applied in this study, the results showed no statistically significant difference between BC and BC/SF:50%. Nevertheless, both materials showed no cytotoxicity and the average cell viability found was  $\mu_{BC} = 91.25\%$ , and  $\mu_{BC/SF:50\%} = 123.81\%$ , respectively. These results are in accordance with ISO standards (10993-5).

#### 3.9.2. Trypan Blue

On the other hand, the cytotoxicity assays related to Trypan Blue dye technique evidenced a statistically significant difference ( $p = 0.02$ ). Dunns post test pointed out that BC/SF:50% group presented a superior performance, indicating less cytotoxicity and a greater number of viable cells compared to the references (Fig. 6).

Although Trypan Blue results differ from those obtained by the MTT assay, both *in vitro* assays evidenced a high cell viability greater than 90% for all treatments, indicating that the material is non-cytotoxic and could allow cell attachment and proliferation. Despite the cytotoxicity results being mutually consistent this difference may occur because Trypan Blue assay measures the cytotoxicity

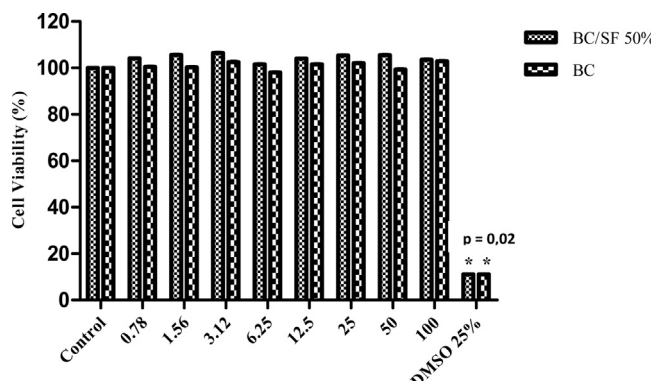


**Fig. 7.** Percentage of cell viability by XTT colorimetric assay in V79 cells. BC – bacterial cellulose, SF – silk fibroin, DMSO – dimethylsulfoxide. \*Statistically different to the negative control.

by cell membrane integrity, while MTT measures the activity of mitochondrial dehydrogenases.

### 3.9.3. XTT assay

The percentage of cell viability found for each treatment is presented in Fig. 7. The results showed that the lyophilized BC/SF:50% as well as BC treatments do not indicate statistically significant differences when compared to the negative control in all concentration tested, revealing the lack of cytotoxicity. Cell viability of the tested material was greater than 95%.

### 3.9.4. Cell adhesion and proliferation

To test the hypothesis that fibroin increases cell adhesion into cellulose scaffolds, L-929 cells were seeded into the pristine BC scaffolds and BC/SF:50% nanocomposite. Cells were lifted up and

counted in hemocytometer chamber. In relation to cell proliferation and adhesion assays the value found was significant at  $p = 0.04$ .

The images of Fig. 8 show that the cells seeded on pure BC and BC/SF:50% scaffolds surface (a, b) did not migrate into the material (c, d). This fact was expected because the dense structure of BC networks displays a pore size not large enough to allow migration and consequently complex 3D scaffolds could not be obtained. (Bäckdahl et al., 2006). However, the presence of SF induced a significant increase in cell adhesion on BC/SF 50% nanocomposites in relation to the pure cellulose scaffolds ( $p < 0.05$ ).

The results provided by cytotoxicity tests added to the analysis of these images indicate that BC/SF:50% composite displays higher cell viability in comparison to pure BC in terms of fibroblast adhesion. The cells observed in pure BC scaffold remained round-shaped whereas the cells that adhered to the BC/SF50% scaffold are completely spread over the surface, with the presence of many pseudopodia forming a layer, suggesting that cells stretching their morphology were proliferating.

It is known that the pore sizes of a scaffold matrix affect the cell adhesion and proliferation. The results obtained in this study related to the porosity of the material were in accordance with the literature; therefore, the BC/SF:50% produced scaffolds could act allowing BMSCs proliferation and ECM production.

However, it is important to point that this improvement in cells proliferation probably occurred due to the peculiar composition of silk fibroin. Fibroin is an insoluble protein containing up to 90% of the amino acids glycine, alanine, and serine that form crystalline  $\beta$ -sheets in silk fibers (Fang, Chen, et al., 2009; Fang, Wan, et al., 2009; Fu et al., 2013). These types of proteins usually exhibit great mechanical properties and, in combination with their biocompatibility, provide an important set of options in the field of controlled release, biomaterials and scaffolds for tissue engineering and medical applications.

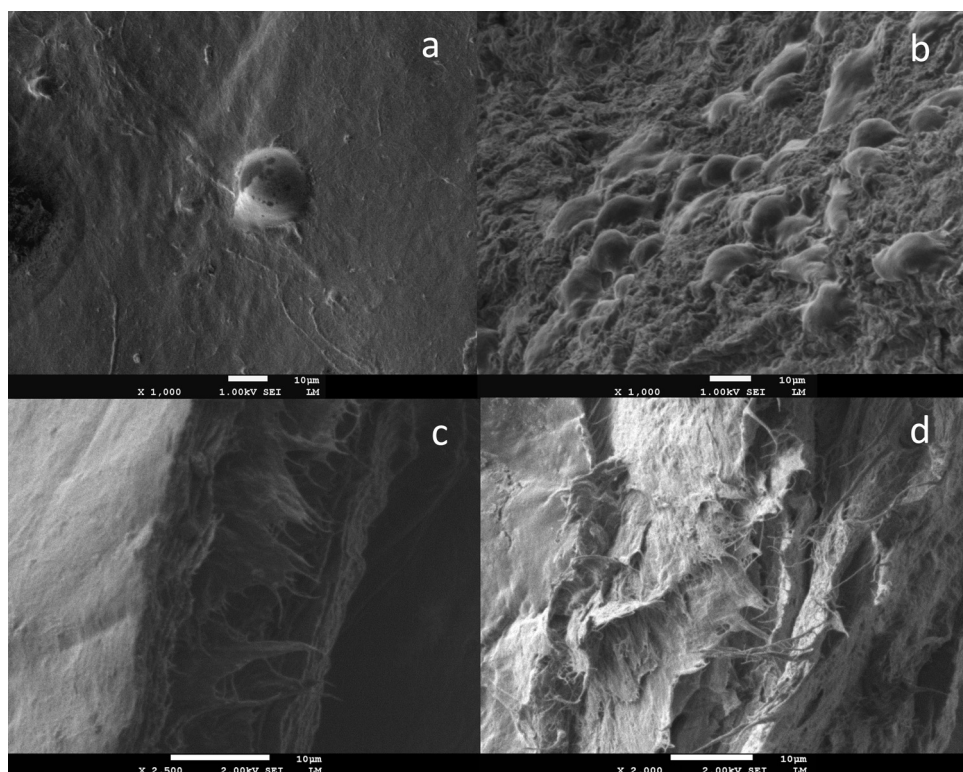


**Fig. 8.** To test the hypothesis that the addition of silk fibroin to cellulose scaffolds increases cell adhesion (48 h), L-929 cells were seeded in BC and BC/SF scaffolds. SEM images of the cells attached to BC (a) and BC/SF (b) scaffolds surface; cross-section SEM images of BC (c) and BC/SF (d) evidenced that the cells did not migrate into the scaffolds.

**Table 1**

Frequencies of micronuclei (MN) and nuclear division index (NDI) obtained in V79 cell cultures treated with BC/SF 50% and respective controls.

Treatments	MN frequency <sup>a</sup> Mean ± SD	NDI <sup>b</sup> Mean ± SD
Negative control	7.33 ± 1.52	1.75 ± 0.02
BC control (100%)	5.66 ± 1.54	1.68 ± 0.01
25%	7.00 ± 2.00	1.68 ± 0.02
50%	5.00 ± 1.00	1.67 ± 0.10
100%	4.66 ± 1.52	1.69 ± 0.05
MMS	90.00 ± 6.00 <sup>c</sup>	1.84 ± 0.02

MMS, methyl methanesulfonate (44 µg/mL).

<sup>a</sup> A total of 3000 binucleated cells were analyzed per treatment group.

<sup>b</sup> A total of 1500 cells were analyzed per treatment group.

<sup>c</sup> Significantly different to the negative control group ( $p < 0.05$ ).

Other studies (Chiarini et al., 2003; Dal Prà et al., 2003; Enomoto et al., 2010; Petrini, Parolari, & Tanzi, 2001) evidenced a few more properties of silk fibroin such as: it can be chemically modified with adhesion sites or cytokines, due to the availability of amine and acid side chains on some of the amino acids; it presents slow rates of degradation *in vitro* and *in vivo*, that is particularly useful in biodegradable scaffolds in which slow tissue ingrowth is desirable.

According to the present findings, BC/SF:50% scaffolds evidenced potential applications in terms of alternative materials for tissue regeneration and medical devices. Further investigation such as differentiation, osteogenic and osteoinductive potential, improvements related to increase BC/SF porosity and controlled release of active ingredients should be conducted. Additionally, tests in an animal model to evaluate the performance of the material in relation to specific tissues of application, are underway. Future steps point to previously mentioned improvements to turn the material into a more complex 3D scaffold for tissue engineering.

### 3.9.5. Assessment of genotoxicity

The micronuclei frequency and NDI obtained in V79 cells treated with BC/SF:50% and respective controls are demonstrated in Table 1. No significant difference in the frequencies of micronuclei were observed between the cultures treated with 25%, 50% and 100% of BC/SF:50% when compared to the negative control, revealing the lack of genotoxic effect. In relation to NDI values, no significant differences were observed between the different treatments and negative control, demonstrating the absence of cytotoxicity.

## 4. Conclusions

Sponge-like nanocomposites based on bacterial cellulose and silk fibroin (BC/SF:25%, BC/SF:50% and BC/SF:75%) were developed in this work. SEM evaluation results exhibit a very well interconnected porous network structure and large aspect of all nanocomposites produced. It could be demonstrated that the presence of fibroin influenced BC/SF scaffolds surface covering and this aspect was affected by fibroin concentration. The best outcome obtained is related to 50% fibroin content, where the equal ratio led to a very good symbiotic effect, preserving the specific properties of BC and SF. Bradford assay demonstrated that BC/SF:50% nanocomposite is stable. The results for cell adhesion assay showed that the presence of fibroin induced a significant increase on cell adhesion (BC/SF:50%) compared to pure BC membranes, due to the biologic nature of SF coating. Cytotoxicity assays demonstrated that the material is non-cytotoxic and Trypan Blue associated to the SEM images revealed that BC/SF:50% scaffolds present higher rates of cellular viability than pure BC. Further, it was found that the prepared BC/SF:50% scaffold led to an improved biocompatibility

compared to pure BC scaffolds, especially concerning biocompatibility and the suitability to induce cell adhesion. Furthermore, the genotoxicity test revealed that the material is non-genotoxic, indicating safety for medical applications. Generally, the POC of the BC/SF composites could be demonstrated; next, more adjustments are required to generate scaffolds for complex tissue engineering.

## References

- Alessandrino, A., Marelli, B., Arosio, C., Fare, S., Tanzi, M., & Freddi, G. (2008). *Electrospun silk fibroin mats for tissue engineering*. *Engineering in Life Sciences*, 8(3), 219–225.
- Altman, G. H., Diaz, F., Jakuba, C., Calabro, T., Horan, R. L., Chen, J., et al. (2003). *Silk-based biomaterials*. *Biomaterials*, 24(3), 401–416.
- Amsden, J., Domachuk, P., Gopinath, A., White, R., Dal Negro, L., Kaplan, D., et al. (2010). *Rapid nanoimprinting of silk fibroin films for biophotonic applications*. *Advanced Materials*, 22(15), 1746–1749.
- Bäckdahl, H., Helenius, G., Bodin, A., Nannmark, U., Johansson, B., Risberg, B., et al. (2006). *Mechanical properties of bacterial cellulose and interactions with smooth muscle cells*. *Biomaterials*, 27(9), 2141–2149.
- Barnes, C., Elsaesser, A., Arkusz, J., Smok, A., Palus, J., Lesniak, A., et al. (2008). *Reproducible comet assay of amorphous silica nanoparticles detects no genotoxicity*. *Nano Letters*, 8(9), 3069–3074.
- Barud, H., Caiut, J., Dexpert-Ghys, J., Messadeq, Y., & Ribeiro, S. (2012). *Transparent bacterial cellulose-boehmite-epoxy-siloxane nanocomposites*. *Composites Part A: Applied Science and Manufacturing*, 43(6), 973–977.
- Barud, H., de Araujo, A., Santos, D., de Assuncao, R., Meireles, C., Cerqueira, D., et al. (2008). *Thermal behavior of cellulose acetate produced from homogeneous acetylation of bacterial cellulose*. *Thermochimica Acta*, 471(1–2), 61–69.
- Barud, H., Ribeiro, C., Crespi, M., Martines, M., Dexpert-Ghys, J., Marques, R., et al. (2007). *Thermal characterization of bacterial cellulose-phosphate composite membranes*. *Journal of Thermal Analysis and Calorimetry*, 87(3), 815–818.
- Barud, H., Souza, J., Santos, D., Crespi, M., Ribeiro, C., Messadeq, Y., et al. (2011). *Bacterial cellulose/poly(3-hydroxybutyrate) composite membranes*. *Carbohydrate Polymers*, 83(3), 1279–1284.
- Bhardwaj, N., & Kundu, S. (2011). *Silk fibroin protein and chitosan polyelectrolyte complex porous scaffolds for tissue engineering applications*. *Carbohydrate Polymers*, 85(2), 325–333.
- Bhardwaj, N., Nguyen, Q. T., Chen, A. C., Kaplan, D. L., Sah, R. L., & Kundu, S. C. (2011). *Potential of 3-D tissue constructs engineered from bovine chondrocytes/silk fibroin-chitosan for in vitro cartilage tissue engineering*. *Biomaterials*, 32(25), 5773–5781.
- Bodin, A., Bharadwaj, S., Wu, S., Gatenholm, P., Atala, A., & Zhang, Y. (2010). *Tissue-engineered conduit using urine-derived stem cells seeded bacterial cellulose polymer in urinary reconstruction and diversion*. *Biomaterials*, 31(34), 8889–8901.
- Bradford, M. (1976). A rapid and sensitive method for the quantitation of microgram quantities of protein utilizing the principle of protein-dye binding. *Analytical Biochemistry*, 72, 248. Available at: [www.ncbi.nlm.nih.gov/pubmed/942051](http://www.ncbi.nlm.nih.gov/pubmed/942051)
- Cai, X. J., & Xu, Y. Y. (2011). *Nanomaterials in controlled drug release*. *Cytotechnology*, 63(4), 319–323.
- Cattaneo, I., Figliuzzi, M., Azzollini, N., Catto, V., Fare, S., Tanzi, M., et al. (2013). *In vivo regeneration of elastic lamina on fibroin biodegradable vascular scaffold*. *International Journal of Artificial Organs*, 36(3), 166–174.
- Chen, G., Ushida, T., & Tateishi, T. (2002). *Scaffold design for tissue engineering macromolecular bioscience*. *Macromolecular Bioscience*, 2(2), 67–77.
- Chiarini, A., Petrini, P., Bozzini, S., Dal Pra, I., & Armato, U. (2003). *Silk fibroin/poly(carbonate)-urethane as a substrate for cell growth: in vitro interactions with human cells*. *Biomaterials*, 24(5), 789–799.
- Choi, Y., Cho, S. Y., Heo, S., & Jin, H.-J. (2013). *Enhanced mechanical properties of silk fibroin-based composite plates for fractured bone healing*. *Fibers and Polymers*, 14(2).
- Czaja, W. K., Young, D. J., Kawecki, M., & Brown, R. M. (2007). *The future prospects of microbial cellulose in biomedical applications*. *Biomacromolecules*, 8(1), 1–12.
- Dal Prà, I., Petrini, P., Chiarini, A., Bozzini, S., Farè, S., et al. (2003). *Silk fibroin-coated three-dimensional polyurethane scaffolds for tissue engineering: interactions with normal human fibroblasts*. *Tissue Engineering*, 9(6), 1113–1121.
- De Salvi, D., Barud, H., Caiut, J., Messadeq, Y., & Ribeiro, S. (2012). *Self-supported bacterial cellulose/boehmite organic-inorganic hybrid films*. *Journal of Sol-Gel Science and Technology*, 63(2), 211–218.
- Eastmond, D., & Tucker, J. (1989). *Identification of aneuploidy-inducing agents using cytokinesis-blocked human lymphocytes and an antikinetochore antibody*. *Environmental and Molecular Mutagenesis*, 13(1), 34–43.
- Enomoto, S., Sumi, M., Kajimoto, K., Nakazawa, Y., Takahashi, R., Takabayashi, C., et al. (2010). *Long-term patency of small-diameter vascular graft made from fibroin, a silk-based biodegradable material*. *Journal of Vascular Surgery*, 51(1), 155–164.
- Fang, Q., Chen, D., Yang, Z., & Li, M. (2009). *In vitro and in vivo research on using Antheraea pernyi silk fibroin as tissue engineering tendon scaffolds*. *Materials Science and Engineering: C*, 29(5), 1527–1534.
- Fang, B., Wan, Y., Tang, T., Gao, C., & Dai, K. (2009). *Proliferation and osteoblastic differentiation of human bone marrow stromal cells on hydroxyapatite/bacterial cellulose nanocomposite scaffolds*. *Tissue Engineering Part A*, 15(5), 1091–1098.

- Fenech, M. (2000). The in vitro micronucleus technique. *Mutation Research*, 455, 81–95.
- Fontana, J., Desouza, A., Fontana, C., Torriani, I., Moreschi, J., Gallotti, B., et al. (1990). Acetobacter cellulose pellicle as a temporary skin substitute. *Applied Biochemistry and Biotechnology*, 24–25, 253–264.
- Fraser, S., Ting, Y., Mallon, K., Wendt, A., Murphy, C., & Nealey, P. (2008). Sub-micron and nanoscale feature depth modulates alignment of stromal fibroblasts and corneal epithelial cells in serum-rich and serum-free media. *Journal of Biomedical Materials Research Part A*, 86A(3), 725–735.
- Fu, L., Zhou, P., Zhang, S., & Yang, G. (2013). Evaluation of bacterial nanocellulose-based uniform wound dressing for large area skin transplantation. *Materials Science & Engineering C-Materials for Biological Applications*, 33(5), 2995–3000.
- Gao, C., Wan, Y., Yang, C., Dai, K., Tang, T., Luo, H., et al. (2011). Preparation and characterization of bacterial cellulose sponge with hierarchical pore structure as tissue engineering scaffold. *Journal of Porous Materials*, 18, 139–145.
- Grande, C., Torres, F., Gomez, C., & Bano, M. (2009). Nanocomposites of bacterial cellulose/hydroxyapatite for biomedical applications. *Acta Biomaterialia*, 5(5), 1605–1615.
- Helenius, G., Bäckdahl, H., Bodin, A., Nannmark, U., Gatenholm, P., & Risberg, B. (2006). In vivo biocompatibility of bacterial cellulose. *Journal of Biomedical Materials Research Part A*, 76(2), 431–438.
- Hutchens, S., Benson, R., Evans, B., O'Neill, H., & Rawn, C. (2006). Biomimetic synthesis of calcium-deficient hydroxyapatite in a natural hydrogel. *Biomaterials*, 27(26), 4661–4670.
- Jonas, R., & Farah, L. (1998). Production and application of microbial cellulose. *Polymer Degradation and Stability*, 59(1–3), 101–106.
- Kim, J., Cai, Z., Lee, H., Choi, G., Lee, D., & Jo, C. (2011). Preparation and characterization of a bacterial cellulose/chitosan composite for potential biomedical application. *Journal of Polymer Research*, 18(4), 739–744.
- Kim, K., Jeong, L., Park, H., Shin, S., Park, W., Lee, S., et al. (2005). Biological efficacy of silk fibroin nanofiber membranes for guided bone regeneration. *Journal of Biotechnology*, 120(3), 327–339.
- Kim, U., Park, J., Kim, H., Wada, M., & Kaplan, D. (2005). Three-dimensional aqueous-derived biomaterial scaffolds from silk fibroin. *Biomaterials*, 26(15), 2775–2785.
- Kim, H., Yoon, S. C., Lee, T. Y., & Jeong, D. (2009). Discriminative cytotoxicity assessment based on various cellular damages. *Toxicology Letters*, 184(1), 13–17.
- Klemm, D., Heublein, B., Fink, H. P., & Bohn, A. (2005). Cellulose: fascinating biopolymer and sustainable raw material. *Angewandte Chemie. International Edition in English*, 44(22), 3358–3393.
- Klemm, D., Schumann, D., Udhardt, U., & Marsch, S. (2001). Bacterial synthesized cellulose – artificial blood vessels for microsurgery. *Progress in Polymer Science*, 26(9), 1561–1603.
- Kweon, H., Ha, H., Um, I., & Park, Y. (2001). Physical properties of silk fibroin/chitosan blend films. *Journal of Applied Polymer Science*, 80(7), 928–934.
- Lee, J., Kim, J., Lee, O., & Park, C. (2013). The fixation effect of a silk fibroin-bacterial cellulose composite plate in segmental defects of the zygomatic arch an experimental study. *JAMA Otolaryngology – Head & Neck Surgery*, 139(6), 629–635.
- Li, G., Liu, H., Zhao, H., Gao, Y., Wang, J., Jiang, H., et al. (2011). Chemical assembly of TiO<sub>2</sub> and TiO<sub>2</sub>Ag nanoparticles on silk fiber to produce multifunctional fabrics. *Journal of Colloid Interface Science*, 358(1), 307–315.
- Lu, Q., Wang, X., Lu, S., Li, M., Kaplan, D. L., & Zhu, H. (2011). Nanofibrous architecture of silk fibroin scaffolds prepared with a mild self-assembly process. *Biomaterials*, 32(4), 1059–1067.
- Luo, H., Xiong, G., Huang, Y., He, F., Wang, W., & Wan, Y. (2008). Preparation and characterization of a novel COL/BC composite for potential tissue engineering scaffolds. *Materials Chemistry and Physics*, 110(2–3), 193–196.
- Mandal, B., Park, S., Gil, E., & Kaplan, D. (2011). Multilayered silk scaffolds for meniscus tissue engineering. *Biomaterials*, 32(2), 639–651.
- Marelli, B., Alessandrino, A., Fare, S., Freddi, G., Mantovani, D., & Tanzi, M. (2010). Compliant electrospun silk fibroin tubes for small vessel bypass grafting. *Acta Biomaterialia*, 6(10), 4019–4026.
- Marelli, B., Alessandrino, A., Fare, S., Tanzi, M., & Freddi, G. (2009). Electrospun silk fibroin tubular matrixes for small vessel bypass grafting. *Materials Technology*, 24(1), 52–57.
- Mauney, J., Nguyen, T., Gillen, K., Kirker-Head, C., Gimble, J., & Kaplan, D. (2007). Engineering adipose-like tissue in vitro and in vivo utilizing human bone marrow and adipose-derived mesenchymal stem cells with silk fibroin 3D scaffolds. *Biomaterials*, 28(35), 5280–5290.
- Ming, J., & Zuo, B. (2012). Silk I structure formation through silk fibroin self-assembly. *Journal of Applied Polymer Science*, <http://dx.doi.org/10.1002/app.36354>.
- Mizuno, S., Watanabe, S., & Takagi, T. (2004). Hydrostatic fluid pressure promotes cellularity and proliferation of human dermal fibroblasts in a three-dimensional collagen gel/sponge. *Biochemical Engineering Journal*, 20(2–3), 203–208.
- Nazarov, R., Jin, H., & Kaplan, D. (2004). Porous 3-D scaffolds from regenerated silk fibroin. *Biomacromolecules*, 5(3), 718–726.
- Nogueira, G., Weska, R., Vieira, W., Polakiewicz, B., Rodas, A., Higa, O., et al. (2009). A new method to prepare porous silk fibroin membranes suitable for tissue scaffolding applications. *Journal of Applied Polymer Science*, 114(1), 617–623.
- Omenetto, F., & Kaplan, D. (2010). New opportunities for an ancient material. *Science*, 329(5991), 528–531.
- Petrini, P., Parolari, C., & Tanzi, M. C. (2001). Silk fibroin-polyurethane scaffolds for tissue engineering. *Journal of Materials Science: Materials in Medicine*, 12(10–12), 849–853.
- Rambo, C., Recouvreux, D., Carminatti, C., Pitlovancic, A., Antonio, R., & Porto, L. (2008). Template assisted synthesis of porous nanofibrous cellulose membranes for tissue engineering. *Materials Science & Engineering C-Biomimetic and Supramolecular Systems*, 28(4), 549–554.
- Rockwood, D., Preda, R., Yucel, T., Wang, X., Lovett, M., & Kaplan, D. (2011). Materials fabrication from *Bombyx mori* silk fibroin. *Nature Protocols*, 6(10), 1612–1631.
- Ross, P., Mayer, R., & Benziman, M. (1991). Cellulose biosynthesis and function in bacteria. *Microbiological Reviews*, 55(1), 35–58.
- Sah, M. K., & Pramanik, K. (2010). Regenerated silk fibroin from *B. mori* silk cocoon for tissue engineering applications. *International Journal of Environmental Science and Development*, 1(5), 404–408.
- Saska, S., Barud, H. S., Gaspar, A. M., Marchetto, R., Ribeiro, S. J., & Messadeq, Y. (2011). Bacterial cellulose-hydroxyapatite nanocomposites for bone regeneration. *International Journal of Biomaterials*, 2011, 175362. <http://dx.doi.org/10.1155/2011/175362>, 8 pp.
- Saska, S., Teixeira, L., de Oliveira, P., Gaspar, A., Ribeiro, S., Messadeq, Y., et al. (2012). Bacterial cellulose-collagen nanocomposite for bone tissue engineering. *Journal of Materials Chemistry*, 22(41), 22102–22112.
- Schmitt, D., Frankos, V., Westland, J., & Zoetis, T. (1991). Toxicologic evaluation of cellulon™ fiber – genotoxicity, pyrogenicity, acute and subchronic toxicity. *Journal of the American College of Toxicology*, 10(5), 541–554.
- Shi, L. B., Cai, H. X., Chen, L. K., Wu, Y., Zhu, S. A., Gong, X. N., et al. (2014). Tissue engineered bulking agent with adipose-derived stem cells and silk fibroin microspheres for the treatment of intrinsic urethral sphincter deficiency. *Biomaterials*, 35(5), 1519–1530.
- Shi, Q., Li, Y., Sun, J., Zhang, H., Chen, L., Chen, B., et al. (2012). The osteogenesis of bacterial cellulose scaffold loaded with bone morphogenetic protein-2. *Biomaterials*, 33(28), 6644–6649.
- Sofia, S., McCarthy, M., Gronowicz, G., & Kaplan, D. (2001). Functionalized silk-based biomaterials for bone formation. *Journal of Biomedical Materials Research*, 54(1), 139–148.
- Svensson, A., Nicklasson, E., Harrah, T., Panilaitis, B., Kaplan, D. L., Brittberg, M., et al. (2005). Bacterial cellulose as a potential scaffold for tissue engineering of cartilage. *Biomaterials*, 26(4), 419–431.
- Ul-Islam, M., Khan, T., & Park, J. (2012). Water holding and release properties of bacterial cellulose obtained by in situ and ex situ modification. *Carbohydrate Polymers*, 88(2), 596–603.
- Wang, Y., Blasioli, D., Kim, H., Kim, H., & Kaplan, D. (2006). Cartilage tissue engineering with silk scaffolds and human articular chondrocytes. *Biomaterials*, 27(25), 4434–4442.
- Yang, C., Gao, C., Wan, Y., Tang, T., Zhang, S., & Dai, K. (2011). Preparation and characterization of three-dimensional nanostructured macroporous bacterial cellulose/agarose scaffold for tissue engineering. *Journal of Porous Materials*, 18(5), 545–552.
- Zeltinger, J., Sherwood, J., Graham, D., Mueller, R., & Griffith, L. (2001). Effect of pore size and void fraction on cellular adhesion, proliferation, and matrix deposition. *Tissue Engineering*, 7(5), 557–572.
- Zhang, Y., Fan, W., Ma, Z., Wu, C., Fang, W., Liu, G., et al. (2010). The effects of pore architecture in silk fibroin scaffolds on the growth and differentiation of mesenchymal stem cells expressing BMP7. *Acta Biomaterialia*, 6(8), 3021–3028.